Argonne National Laboratory

PHYSICS DIVISION

SUMMARY REPORT

January 1962

ARGONNE NATIONAL LABORATORY
9700 South Cass Avenue
Argonne, Illinois

PHYSICS DIVISION
SUMMARY REPORT

January 1962

Morton Hamermesh, Division Director

Preceding Summary Reports:

ANL-6391, July-August 1961
ANL-6432, September-October 1961
ANL-6455, November-December 1961

FOREWORD

The Summary Report of the Physics Division of the
Argonne National Laboratory is issued monthly for the information of
the members of the Division and a limited number of other persons
interested in the progress of the work. Each active project reports
about once in 3 months, on the average. Those not reported in a
particular issue are listed separately in the Table of Contents with a
reference to the last issue in which each appeared.

This is merely an informal progress report. The
results and data therefore must be understood to be preliminary and
tentative.

The issuance of these reports is not intended to con-
stitute publication in any sense of the word. Final results either
will be submitted for publication in regular professional journals or,
in special cases, will be presented in ANL Topical Reports.

TABLE OF CONTENTS

The date of the last preceding report is indicated after the title of each project below. Projects that are not reported in this issue are listed on subsequent pages.

V. THEORETICAL PHYSICS, GENERAL

PROJECTS NOT REPORTED IN THIS ISSUE

A reference to the last preceding report is given in parentheses for each project.

I. EXPERIMENTAL NUCLEAR PHYSICS

I-3. Cross Section Measurements with the Fast Neutron Velocity Selector (ANL-6072, October-November 1959), L. M. Bollinger and R. E. Cote'.

I-9. Lifetimes of Energy Levels Excited by Slow-Neutron Capture (ANL-6326, March 1961), L. M. Bollinger.

I-10. Tandem Van de Graaff Accelerator (ANL-6262, December 1960), F. P. Mooring and J. R. Wallace.

I-14. Pulsed Beams for the Van de Graaff Machine (ANL-6391, July-August 1961), R. E. Holland.

I-18. Differential Cross Sections for Neutron Resonance Scattering (ANL-6455, November-December 1961), R. O. Lane.

I-19. Nuclear Resonance Absorption of Gamma Rays (ANL-6455, November-December 1961), L. L. Lee, Jr., L. Meyer-Schützmeister, and J. P. Schiffer.

I-22. Scattering of Charged Particles (ANL-6455, November-December 1961), J. L. Yntema, B. Zeidman, and T. H. Braid.

I-28. Angular Correlations in Charged-Particle Reactions (ANL-6358, April-May 1961), T. H. Braid.

I-34. Decay of $_{68}Er^{172}$ (ANL-6432, September-October 1961), S. B. Burson and R. G. Helmer.

I-35. Decay of $_{57}La^{135}$ (19.5 hr) (ANL-6391, July-August 1961), S. B. Burson and H. A. Grench.

I-55. Capture Gamma-Ray Spectra for Neutrons with Energies from 0.1 to 10 ev (ANL-6052, September 1959), S. Raboy and C. C. Trail.

II. MASS SPECTROSCOPY

III. CRYSTALLOGRAPHY

I.   EXPERIMENTAL NUCLEAR PHYSICS

I-11-30   Installation and Operation of the Van de Graaff Generator
                                                                        (51210-1)
                    Jack R. Wallace

This report covers the operation of the 4.5-Mev Van de Graaff generator in the Physics Division for the period from October 1 to December 31, 1961, inclusive.

Protons, alphas, and deuterons were accelerated by the generator. The terminal voltage of the Van de Graaff during this period was varied from 0.8 Mv to 4.4 Mv. Beam currents measured at the experimenters target varied from 0.1 μa to 25.0 μa.

Below is a list of experiments being performed with the beams from the generator and the experimenters associated with these experiments.

1. Alpha-gamma reactions	Lee, Meyer-Schützmeister, Malik, Weinman	227.8 hr
2. Investigation of energy levels in B^{10}	Popic	118.4
3. (d, α) reactions	Schiffer, Lee, Braid	45.2
4. Sputtering experiments in Rutherford collision region	Kaminsky	99.6
5. Lifetime of excited states	Lynch	110.7
6. Elastic scattering of protons	Mertz	55.3
7. Neutron polarization	Elwyn, Lane, Langsdorf	129.8
8. (p, γ) and (p, p'γ)	Lee	58.3
	Running time	845.1 hr
	Start up and daily maintenance	43.0
	Generator repairs and experimental setups	303.9

Total time available (63 days × 16 hr/day + 23 days × 8 hr/day) 1192.0 hr

The operational failures of the generator were routine in nature during this period. No major changes were made on the generator.

The charging belts used in the Van de Graaff are now put into a metal container connected to a high-vacuum pumping system with a liquid nitrogen trap. The purpose is to remove any water or other condensible vapors that are present on the belt. Although no detailed tests have been made, we believe this has improved their performance. Belts that originally failed to perform properly in the generator have been satisfactory after this treatment. All belts now get this treatment and are stored in evacuated containers.

II. MASS SPECTROSCOPY

II-23-1 Sputtering Experiments in the Rutherford Collision Region

(51300-01)

M. Kaminsky

Sputtering phenomena have been studied by many authors[1] in the hard-sphere collision region and to a lesser extent in the region of weakly screened Coulomb collisions. For the energy region above 100 kev, where for light incident ions ($Z_1 \leqslant 2$) bombarding targets with $Z_2 < 40$ the Rutherford scattering predominates, the only data for "back" sputtering[2] known to the author are preliminary results reported by Pleshivtsev.[3] However there exists a discrepancy of 3 to 4 orders of magnitude between sputtering ratios reported by this author for deuterons bombarding a copper target and the theoretical predictions for the same system, such as those of Goldman and Simon,[4] Goldman, Harrison, and Coveyou,[5] Harrison, and Pease.[7] It seemed interesting, therefore, to check the experimental result by experiments in the Rutherford collision region. Such collisions,

---

[1] M. Kaminsky, review article for Ergeb. exakt. Naturwiss. (in preparation). For data up to 1955, see the article by G. K. Wehner, Adv. in Electr. Phys. 7, 289 (1955).

[2] It is necessary to discriminate between "back" sputtering and "forward" sputtering. In back sputtering the target particles leave from the surface that is struck by the incident ion beam, while in forward sputtering they leave from the opposite surface [see experiments by M. W. Thompson, Phil. Mag. 4, 139 (1959)].

[3] N. V. Pleshivtsev, Soviet Phys. JETP 37, 882 (1960).

[4] D. T. Goldman and A. Simon, Phys. Rev. 111, 383 (1958).

[5] D. T. Goldman, D. E. Harrison, and R. R. Coveyou, Oak Ridge National Laboratory Report 2729 (1959).

[6] D. E. Harrison, J. Chem. Phys. 32, 1332 (1960).

[7] R. S. Pease, Rendiconti S.I.F., Corso XIII, September 1959, p. 158.

4

which displace target atoms, occur when the energy E of the incident ions is greater than a limiting energy[8]

$$E_B = 4E_R^2 Z_1^2 Z_2^2 (Z_1^{2/3} + Z_2^{2/3}) \frac{M_1}{M_2} \frac{1}{E_d} , \tag{1}$$

where M_1, Z_1 and M_2, Z_2 are the mass and the atomic number of the incident ion and the target atom, respectively, $E_R = 13.6$ ev is the Rydberg energy for hydrogen, and E_d is the energy required to displace an atom from its lattice site. For many metals the values of E_d are 20-25 ev (e.g., $E_d = 25$ ev for Cu and 21 ev for Ag).

In our experiments two single crystals of electrolytic copper, $\frac{1}{4} \times \frac{1}{4} \times 1$ in., were bombarded under normal incidence with deuterons with energies of 0.8 — 2.5 Mev. The surface bombarded was the (110) plane of one crystal and the (100) plane of the other. These crystallographic planes were parallel within 3° to the actual target plane, as determined by Laue diagrams. In a cycle, repeated three times, the surfaces were polished mechanically and very slightly etched. The crystals were dipped for about 1 min into the etching bath, consisting of 25% acetic acid, 55% ortho phosphoric acid, and 20% nitric acid. The surfaces obtained had a mirror finish and were examined by optical and electron microscopy before and after the bombardment. The appearance of pits in the surface could be observed after the bombardment. The results of such surface "etch effects" will be reported elsewhere. Before the crystal was mounted in the target holder, the surface was freed of adherent traces of the replicating plastic by swabbing with tri-chlor ethylene, acetone, and methyl alcohol. The experimental arrangement is shown schematically in Fig. 1. The target chamber shown schematically in Fig. 2 was fitted with a triple bellows system by which the
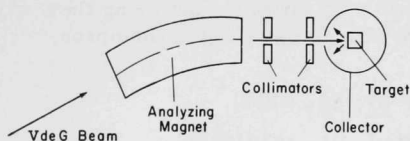
Fig. 1. Schematic diagram of the experimental arrangement.

---

[8] N. Bohr, Kgl. Danske Videnskab. Selskab, Mat. – fys. Medd. 18, 8 (1948).
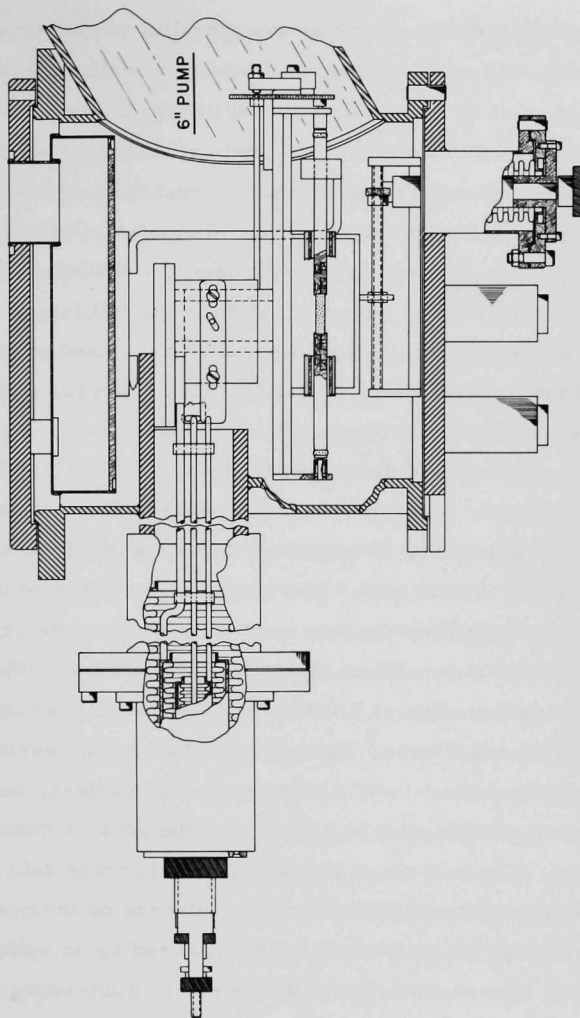
Fig. 2. Schematic drawing of the target chamber. A is the triple bellows
system for the target movements. B is the quartz collector. C is the
target. D are Kovars for electrical connections. E is a single bellows
system for shifting the quartz collector. F is the outlet for the 6-in.
mercury diffusion pump. G is a liquid nitrogen trap, to which fingers
are attached to cool the target. The target chamber is made of Inconel
and gold gaskets are used for sealing.

crystal could be rotated around an axis parallel to the surface plane under bombardment, and moved horizontally and vertically in a plane perpendicular to the direction of the incident beam. With this arrangement the sputtering could be studied as a function of the angle of incidence and a fresh target spot could be bombarded in each run. Around the target was a collector consisting of a quartz tube with an inner diameter of 18 mm and a length of 100 mm. In order to pass the incident beam, a slit about 3 mm wide and parallel to the axis of the tube was cut down the full length. Another bellows system (see Fig. 2) allowed the collector to be shifted parallel to the axis of rotation of the crystal. This exposed a fresh collector surface for each sputtering experiment without opening the machine.

A beam of deuterons from the Van de Graaff passed through an analyzing magnet and two collimating plates before striking a target spot about 2 mm in diameter. The current densities for different runs ranged between 300 and 600 $\mu A/cm^2$. The measured total target current was corrected for the secondary electron current in order to determine the actual beam current. The secondary electrons made up about 10% of the total current, the contribution at 2.0 Mev being about 25% less than at 0.8 Mev. Aarset, Cloud, and Trump[9] have observed a similar variation of the secondary emission from Ni and Au bombarded by protons, but their secondary currents were considerably larger than in the present experiments.

The vacuum in the target chamber was held at 2×10^{-7} mm Hg. The sputtered target atoms were condensed on the quartz wall. The relative thickness of the deposits was measured by an optical transmission method using a monochromatic light source (sodium vapor lamp), a sapphire light pipe, and a photomultiplier arrangement. The data taking was automated by using a motor-driven collector and registering the photocurrents on a chart recorder. The relationship between the transparency of the deposits and the layer thickness was taken from Koedam's data.[10] A layer 30 A thick is still detectable. A mass spectrometer now under construction will serve as a more sensitive detector and will distinguish the different

[9] B. Aarset, R. W. Cloud, and J. G. Trump, J. Appl. Phys. 25, 1365 (1954).

[10] M. Koedam, Thesis, State University of Utrecht, March, 1961.

species of sputtered particles (ions, atoms, or molecular species). However, the deposition of the sputtered particles on a transparent collector has the advantage of showing their angular distribution.

Our measurements indicate that the angular distribution does not follow a cosine law but is more peaked in the direction normal to the surface, and approaches the cosine distribution only for angles larger than 40° from this normal. The deposit appeared to show a faint spot pattern corresponding to the preferred ejection of atoms along close-packed crystal directions. In the case of the (100) crystal plane, the contribution of the (110) directions seemed to show up under 45° but was too thin for a definite identification. Because of the width of the slit in the collector and the diffraction effects at the edges of the slit, the deposits could be detected accurately only for angles larger than 25° with respect to the normal.

The observed deviations from the cosine distribution do not allow the determination of a "uniform" sputtering ratio. The first exploratory experiments were conducted by bombarding a (110) plane of a copper single crystal successively with 0.80- and 2.5-Mev deuterons. The chosen period of irradiation was too short to allow more than an upper limit $S_{max} = 5 \times 10^{-2}$ to be set for the sputtering ratio at each energy. Since these results indicated a ratio approximately two orders of magnitude lower than Pleshivtsev's, an absolute value for the sputtering ratio was sought. For 800-kev deuterons bombarding a (100) plane of a copper single crystal, the sputtering ratio was found to be $S = 1.1 \times 10^{-3}$ atom/ion at 25° and 5.8×10^{-4} atom/ion at angles larger than 40°. The results at these two angles are shown in Fig. 3 as two dots connected by a solid line. For the case of 1.5-Mev deuterons bombarding the same single-crystal plane, the limited irradiation time allowed establishing only an upper limit $S_{max} = 0.9 \times 10^{-3}$ atom/ion. As shown in Fig. 3, these values of the sputtering ratios are 3 to 4 orders of magnitude smaller than those reported by Pleshivtsev. The present results indicate also that the sputtering ratio decreases with increasing energy, contrary to the findings of Pleshivtsev.

8
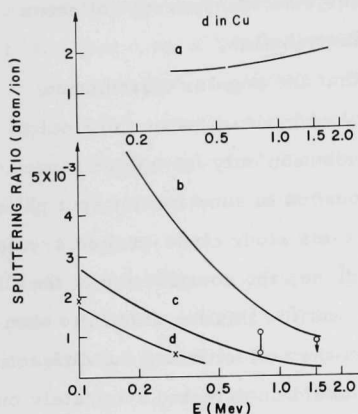
Fig. 3. Comparison of sputtering ratios for deuterons bombarding copper under normal incidence. Curves a, b, c, and d represent the values from references 3, 7, 4, and 5, respectively. The points marked + in curve d are from reference 6. The two dots connected by a solid line represent the values determined from the deposits collected at angles of 25° (S= 1.1 ×10^{-3}) and larger than 40° (S=5.8 × 10^{-4}) when the (100) plane of a copper single crystal was bombarded with 0.8-Mev deuterons. The established upper limit of the sputtering ratio for 1.5-Mev deuterons is also shown by a dot.

Unfortunately, Pleshivtsev did not state the experimental conditions under which he obtained his results. However, the high values of the sputtering ratio and their increase with increasing energy seem to indicate that an evaporation process is superimposed on the sputtering process. Such target evaporation becomes likely if the power transmitted by a high-energy beam at large ion currents is too great to be dissipated rapidly enough by a thin target (e.g., a foil or film).

It seems of interest to compare the present results with values calculated on the basis of different theoretical concepts and to discuss briefly a sputtering model which seems to be plausible for the energy region considered. Consider a Rutherford collision in which an incident particle penetrates the target where its mean free path is λ (about 0.8 ×10^{-4} cm for 500-kev deuterons on Cu) and displaces a target atom from its lattice site as a "primary knock-on." The cross section σ_d for such collisions for $E > E_B$ has been given by Bohr[8] as

$$\sigma_d = 4 \frac{M_1}{M_2} Z_1{}^2 Z_2{}^2 E_R{}^2 \left(1 - \frac{E_d}{\Lambda E}\right) \frac{\pi a_0{}^2}{E_d E} , \qquad (2)$$

where $\Lambda = 4M_1 M_2 / (M_1 + M_2)^2$ and a_0 is the Bohr radius. The mean energy $\overline{E}$ of these "primary knock-ons" is

$$\overline{E} = E_d \ln \frac{E_{max}}{E_d} , \tag{3}$$

with

$$E_{max} = \frac{4M_1 M_2}{(M_1 + M_2)^2} E.$$

If the condition $\overline{E} \ll E_{max}$ is fulfilled, the primary knock-ons are displaced normal to the direction of incidence. These primary knock-ons in turn interact with neighboring lattice atoms by hard-sphere collisions and produce secondary displacements. Such successive collisions continue until the displaced atoms have cooled to such an extent that their kinetic energies have fallen to the order of the displacement energy. A certain fraction of these displaced particles will have a chance to reach the surface and to escape. Several authors tried, on the basis of different concepts, to relate the number of sputtered atoms to the number of such displaced target atoms. Certain simplifying assumptions are commonly made in all these theories. For instance the anisotropy of the energy transfer within the lattice is neglected, as is the electron excitation as a principal mode of energy loss for fast-moving charged particles in a solid [whenever $E > E_c = \frac{1}{16} (M_1 / m_e) W_i$, where W_i is the Fermi energy of the free electrons and m_e is the electron mass]. For d on Cu, $E_c = 1.1$ kev. As long as $\overline{E} < E_c$, this effect will be important only for the energy loss of the incident particle.

Goldman and Simon[4] assumed that the production of primary knock-ons is inversely proportional to the mean free path λ of the incident particle. The subsequent secondary collisions were treated as hard-sphere interactions and the sputtering ratio S was assumed to be also proportional to the average number $\overline{\nu}$ of displaced secondary atoms. Under simplified assumptions, corrections were made for displaced target atoms which got trapped in the lattice. According to the authors, the expression for the sputtering ratio S is

$$S = \frac{k \bar{v}}{\lambda} , \tag{4}$$

where $k = 0.17/\sigma_d$, in which $\sigma_d = \pi R^2$ is the cross section for hard-sphere collisions. By inserting the proper expressions for λ and $\bar{v}$ into Eq. (4) as described by Seitz and Koehler[11] for the energy region considered, the authors obtain

$$S = 0.17\bar{v} \; \frac{Z_1^2 Z_2^2 e^4}{E \, E_d R^2} \; \frac{M_1}{M_2} \; \frac{1}{\cos \psi} , \tag{5}$$

where $\bar{v} = [\, 0.885 + 0.561 \ln \frac{1}{4} (x + 1)] \; (x+1)/x$, with

$$x = \frac{4M_1 M_2}{(M_1 + M_2)^2} \; \frac{E}{E_d} .$$

Here ψ is the angle of incidence and the other notations are the same as used in Eqs. (1) - (3). Calculated values for S (E), based on Eq. (5) for a copper target bombarded by deuterons, are plotted as curve c in Fig. 3.[5]

Applying the same model, Goldman, Harrison, and Coveyou performed a Monte Carlo calculation and obtained the results shown as dots in curve d in Fig. 3. A comparison between curves c and d shows a qualitative agreement for the function S (E), but quantitatively the sputtering ratios plotted in curve d are smaller than those in curve c.

Harrison[8] used a modified model to derive an analytical expression which includes the equation of Goldman and Simon as a special case. The sputtering ratios calculated from Harrison's theory are also shown on curve d of Fig. 3.

According to Pease,[7] the sputtering ratio S is determined by three factors. One is the effective collision area available within one layer $(S \propto \sigma_d n^{2/3})$, a second is the number of layers contributing to sputtering $(S \propto 1 + N^{1/2})$, and the third is the total number of displaced atoms per primary knock-on $(S \propto \frac{1}{2} \bar{E}/ 2E_d)$. Thus the sputtering ratio for normal incidence and for $2E_d < \bar{E} < E_{max}$ is given by

[11] F. Seitz and J. Koehler, Solid State Phys. 2, 307 (1956).

$$S = \sigma_d n^{2/3} (1 + N^{1/2}) \frac{1}{4} \frac{\overline{E}}{E_d} . \tag{6a}$$

Here σ_d is the displacement cross section for the energy region considered, n is the number of target atoms per unit volume, and N is the number of hard-sphere collisions the primary knock-ons make with other atoms in slowing down to an energy E_s corresponding to the heat of sublimation of the target. If binary collisions are assumed in a random-walk calculation,[12] the total number of atomic layers (including the surface layer) contributing to sputtering is found to be

$$1 + N^{1/2} = 1 + \left[\frac{\log (\overline{E}/E_s)}{\log 2} \right]^{1/2} .$$

By inserting this into equation (6a) one gets

$$S = \sigma_d n^{2/3} \left[1 + \frac{\log (\overline{E}/E_s)}{\log 2} \right]^{1/2} \cdot \frac{1}{4} \frac{\overline{E}}{E_d} . \tag{6b}$$

On the basis of Eq. (6b) Pease calculated values for the sputtering ratio S of copper targets bombarded by protons, deuterons, and helium ions. Curve b in Fig. 3 represents such calculated values for deuterons bombarding copper. (Values are taken from Fig. 1 of Pease's article.) A comparison of curves b, c, and d shows that the values calculated by Pease are considerably larger than the ones calculated by other authors.[4-6] However all three curves predict a decrease of the sputtering ratio with increasing energy.

Contrary to these calculations, Pleshivtsev predicted that the sputtering ratio should increase with increasing energy in the considered energy region $E > E_B$. He tried to correlate the sputtering ratio with the total number of displaced particles, a number which will actually increase with increasing energy. However, as mentioned above, only a fraction of the total number of displaced particles will have a chance to

[12]
S. Chandrasekhar, Revs. Modern Phys. 15, 12 (1943).

reach the surface and to escape. Pleshivtsev's values of the sputtering
ratios are therefore larger than those predicted by other authors.
Pleshivtsev's values for the sputtering of copper by deuterons are given
in curve a in Fig. 3. The values in curve a are 3 to 4 orders of magnitude
higher than those in b, c, and d and they increase with increasing energy.

    In conclusion, the experimentally determined sputtering
ratios presented here lie between those calculated by Goldman and Simon[4]
and Pease[7] and agree with them within a factor of two; but they disagree
with those reported by Pleshivtsev by 3 to 4 orders of magnitude. The
data also show a decrease of the sputtering ratio with increasing ion energy,
in qualitative agreement with theoretical predictions[4-7] but contrary to the
findings of Pleshivtsev. Therefore on the basis of these results Pleshivtsev's
claim that the theory of Goldman and Simon is "incorrect in general" does not
seem justified. Furthermore, the present results indicate that the distribu-
tion of the sputtered particles deviates from a cosine distribution in the energy
range investigated.[13] This makes a definition of the sputtering ratio de-
pendent on the direction of the escaping target atoms.

    Further experiments will be conducted with protons, deuterons,
and helium ions bombarding copper and silver single crystals at different
angles of incidence in the energy range from 100 to 200 kev and 0.8 to 4.0
Mev with the present experimental setup as well as by a mass spectrometric
method.

---

[13]
    For corresponding results for low-energy sputtering, see the work of
G. K. Wehner [J. Appl. Phys. 31, 177 (1960)] . More references are given
there.

II-39-1   Fragmentation of Cyanogen   (51310-01)

H. E. Stanton

ENERGY DISTRIBUTION OF IONS FROM C_2N_2

This study was initiated in response to a recent request for an energy analysis of the positive ions of mass 26 (CN^+) formed in the electron bombardment of cyanogen (C_2N_2). In order to monitor the operation of the mass spectrometer (MA-17) it was necessary to use a suitable standard with which to compare the peak shape of the unknown. The standard used was the parent ion of argon. During the investigation, a lower limit was determined for the resolution width of the instrument. The purpose of this report is to present the partial results for cyanogen and this rather important parameter of the instrument.

The calculated "temperature,"[1] obtained by a least-squares fitting of the experimental energy distribution with a Maxwell-Boltzmann distribution, was 0.14 ev for the cyanogen fragment peak of mass 26^+. This is to be compared with an "argon temperature" of about 0.05 ev in the calibrating runs. The two energy distributions, as recorded by the mass spectro meter, were markedly different in appearance and there seemed to be no question that the fragment of mass 26^+ was formed with some ions having kinetic energies up to 0.5 ev or more. A direct comparison of the two distributions is shown in Fig. 4.

Fig. 4. Kinetic energy distribution of the fragment of mass 26 (cyanogen), superposed on the distribution in kinetic energy of the parent ion (40^+) from argon. These were direct tracings from the output of the recorder. It is evident that the $C_2H_2^+$ peak from cyanogen has kinetic energy up to roughly 0.5 ev.
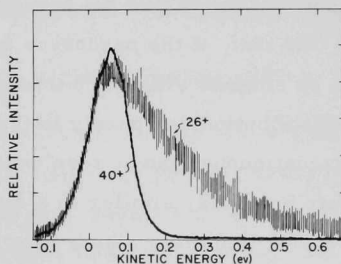
[1] H. E. Stanton, Physics Division Summary Report ANL-5955 (December 1958-January 1959), p. 36.

Comparison of most of the fragment peaks from cyanogen with the peaks of argon ions showed that these fragments were formed with measurable kinetic energies. During the experiment, it was evident that the samples had become contaminated with air so the measurements of masses $m/e = 28^+$ and $m/e = 14^+$ were completely meaningless. The fragment of $m/e = 28^+$ is, apparently, not formed from cyanogen under electron impact. It appeared to be impossible to find a set of initial parameters that would lead to a theoretical fit to the experimental distribution for C^+ and thereby determine its temperature. Consequently, only the experimental curve is shown in Fig. 5. There appears to be a group of ions with energies of about 0.5 ev in addition to those formed with low energies. By comparison with the distribution for C_2N^+, one might estimate the "temperature" as about 0.1 ev.
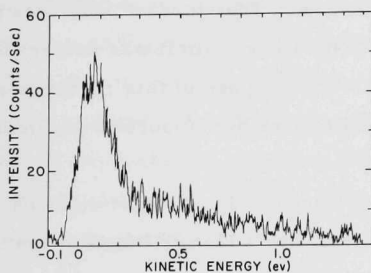
Fig. 5. Kinetic energy distribution of the fragment C^+, directly as recorded. It seemed to be impossible to obtain a set of parameters to give a least-squares fit to a Maxwell-Boltzmann distribution.

Theoretically, the use of a Maxwell-Boltzmann distribution as a basis for fitting the experimental traces is improper except for the parent ion. It is clear from Fig. 4 that the distributions of kinetic energies for CN^+ and A^+ are almost identical for indicated energies below the distribution maxima. This would imply that the precursors for both ions were at thermal energies, .nd that, if the precursor for CN^+ were at rest, the fragment would still be emitted with a kinetic energy distribution. One would surmise that the distribution due purely to the fragmentation would be characterized by a discontinuous rise at zero energy and then a gradual decrease toward higher energies, similar to a single "saw-tooth." This type of kinetic energy distribution, which approximates that generated by some diatomic

fragmentations, is not a proper Maxwell distribution, and requires additional theoretical analysis. The results of the present analysis are summarized in Table I.

TABLE I. Energies of cyanogen fragments formed by impact of electrons with energies of 500-700 ev.

m/e	Fragment	Temperature(ev)
38	C_2N^+	0.099
12	C^+	--
14	N^+	--
20	A^{++}	0.046
40	A^+	0.054
24		0.108
26	CN^+	0.173
		0.109
28	N_2^+	0.049
40	A^+	0.048
40	A^+	0.067
52	$C_2N_2^+$	0.050
		0.059

ENERGY RESOLUTION OF MASS SPECTROMETER

Subsequently, it seemed desirable to try to determine the lower limit of the energy difference the instrument could effectively resolve. This was done by comparing two kinetic energy distributions with the same distribution law but having a known difference in average energy, in order to find what difference in "temperature" might be detectable and

to gain some indication of the reliability of this difference. The results indicate that, with careful operation, differences in "temperatures" of about 0.05 ev are measurable with a reasonable amount of confidence. It had not been anticipated that the mass spectrometer would be able to make a direct measurement of the thermal distribution in a gas at room temperature ($\approx$ 0.025 ev) but the results of the investigation showed that this was probably not impossible, although the accuracy would be low.

The additions to the usual arrangement of the source consisted in providing the ion box (shown in Fig. 6) with an electric heater and a calibrated thermocouple to permit the control and measurement of the ion-box temperature. The heater was supplied with alternating current through an isolation transformer and variable-voltage source, and temperatures were read from a microammeter mounted outside of the vacuum.

Approximately 60 distributions of kinetic energy of A^+ were measured as the temperature of the ion box was varied from about $300^{\circ}K$ to about $550^{\circ}K$ and these runs were then reduced by the IBM-704 to determine the parameters of the distributions, one of these being the "temperature." Electrons with 700 ev energy were used to form the ions. Initial ion acceleration was 200 ev and the total ion acceleration was 8 kv.

The results are shown in Fig. 7 in which the "temperature" as measured by the kinetic energy distributions is plotted as a function of temperature of the ion box as indicated by the thermocouple.

Any correlation between kinetic energy "temperatures" and true
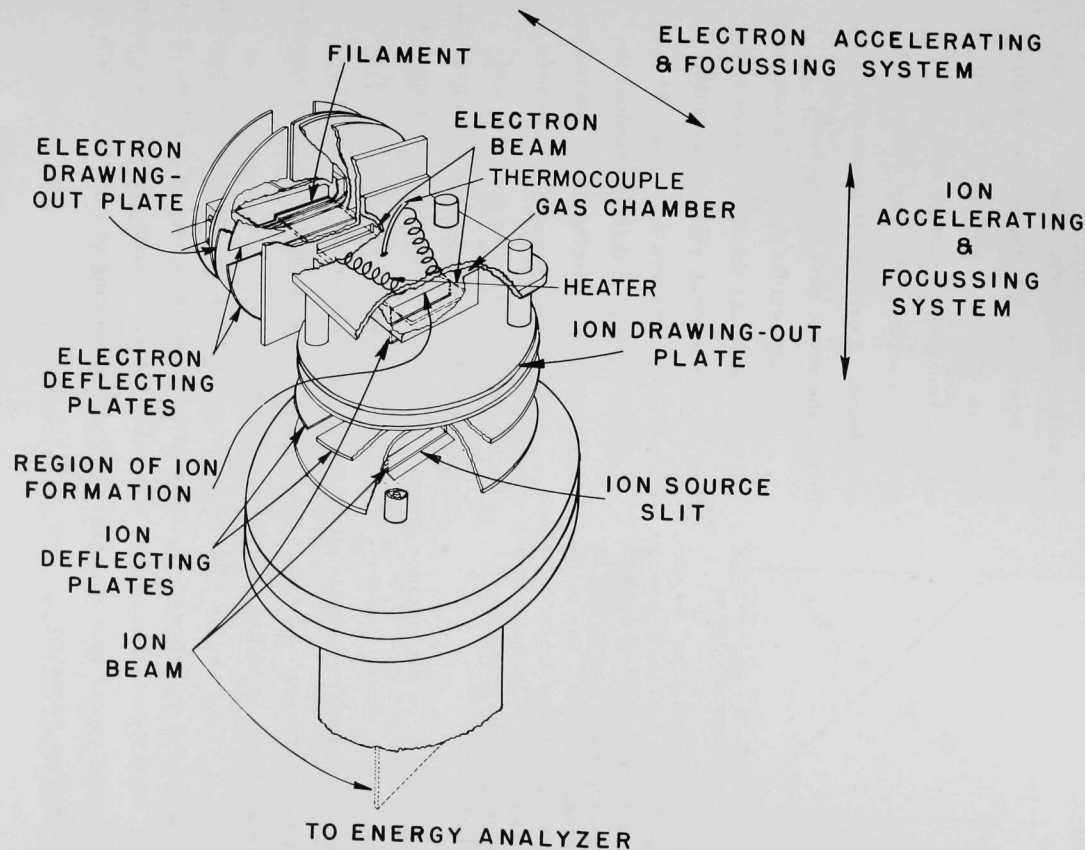
Fig. 6. Source structure used for the analyses. This supplied a focused electron beam transverse to the ion beam in the ion chamber. The figure presents a perspective view of both beams and the structure.

18
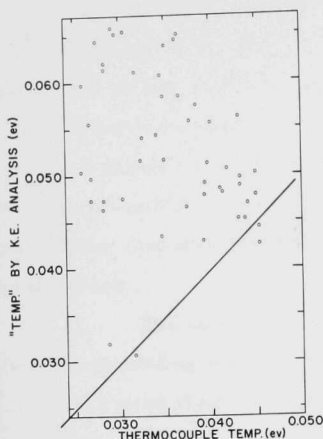
Fig. 7. "Temperatures" as ob-
tained from the kinetic energy
distribution, plotted against
the temperature recorded by
the thermocouple. The points
show all the data taken during
the analysis. The solid line
represents the theoretical
relationship.

temperatures as judged by Fig. 7 is
highly tenuous and, if existent, would
appear to be negative. The curve does
show, however, that the maximum de-
viation is < 0.05 ev and in this sense
a lower limit to the energy difference
the mass spectrometer can resolve has
been found. For this set of runs, however,
this is the worst possible picture.

It was evident during the course of
the measurements that there were inter-
mittent shifts which were occasionally
very troublesome and annoying. At pre-
sent it is suspected that mechanical in-
stability in the mounting of the source or
accelerating structures may have been
one of the causes. The possibility of
electronic misbehavior is always present.
Even pressures on the machine frame, or vibration of the foundation cannot
be excluded as possible causes. It is also pertinent to note that almost all
of the experimental points lie above the theoretical curve. This seems to
imply that any disturbance impairs the energy resolution of the mass spectro-
meter and leads to higher calculated temperatures.

Four or five runs were discarded from the complete set because
the resulting distributions unquestionably showed some type of machine distur-
bance. Usually this disturbance was exhibited as a sudden shift in the energy
which would appear as a sharp discontinuity amounting to from 5% to 100% of
the maximum intensity.

Fig. 8. Same as Fig. 7,
except that the points
shown are from only
a single sweep in ion-
box temperature.
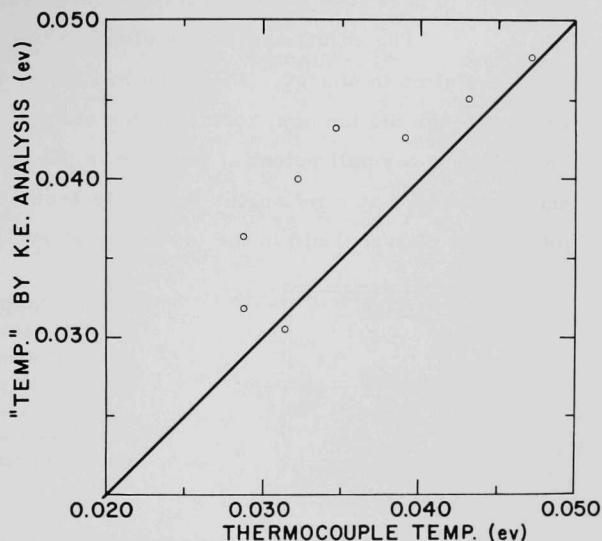
In. Fig. 8, the points of a selected set of runs is shown as
in Fig. 7. The points represent one excursion in the true temperature
of the ion box from about $35^{\circ}C$ to about $240^{\circ}C$ and back. All runs were
made on the same day, and no adjustments were made on either the electron
focusing or the ion focusing. No discontinuous jumps were observed in the
data, and the machine appeared to operate stably throughout. The points
seem to fit the theoretical values surprisingly well. The two points shown
at the temperature of 0.0287 ev represent two values calculated from the
same set of data. The difference arises from the fact that permitted errors
in the iterative calculations were large enough to accommodate both values
as final answers.

A final run was made for mass 26^{+} from cyanogen to give
assurance that the energy transmission of the mass spectrometer was

sufficient to pass ions with appreciable energies.

The adjustment of the electron beam is quite critical for high resolution in energy. As shown in Fig. 6, the electrons pass "sidewise" through the ion box, forming ions along their paths. These ions are drawn out by a small potential gradient in the direction of the ion beam and, therefore, at right angles to the electron beam. An approximate map of the electric field in the ion box is shown in Fig. 9.
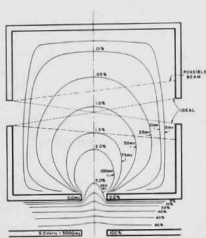
Fig. 9. Map of equipotential lines in a cross-sectional view of the ion box. It was assumed that the difference in potential between the ion chamber and the first ion-drawing-out plate was 5.0 ev, close to the experimental value.

It is clear that the energy possessed by an ion entering the energy selector is determined by any kinetic energy released in its formation and by the difference in potential between its point of formation and the entrance to the energy selector. Consequently, in a poorly defined electron beam, ions will be formed at different physical depths in the ion box and will be at different potentials. Also if a well-defined electron beam is displaced laterally in the ion box, the apparent energy of the ions will be changed. The discontinuous shifts mentioned earlier can, in fact, be explained in this way. For many of the runs plotted in Fig. 7 it became necessary to readjust the electron focus ring, or the ion focusing either because of potential drifts, or because of thermal distortion in the source as a result of the heating, and consequently the potentials at which the ions were formed were changed, or the electron beam broadened. Since variations of a few millivolts are involved, the scatter in the points in Fig. 7 is not surprising. Actually, the consistency of the points in Fig. 8 is surprising and probably somewhat fortuitous. The slope of the curve, as shown in Fig. 8, was not confined to that set of runs. Several other sequences

of runs which form a part of Fig. 7 showed the same slope, i.e., varia-
tions which were paralled to the theoretical line, but displaced from it.
Consequently, the measurement of temperature changes can be made
with greater precision than the absolute value. During normal operation
of the mass spectrometer, it is customary to compare the "temperature"
of an unknown peak with a standard. As a result of the measurements re-
corded here, it is reasonable to expect that "temperature" differences be-
tween an unknown ion and a standard ion will indicate kinetic energies of
formation with an uncertainty of less than 0.05 ev according to the "tem-
perature" model.

Efforts to eliminate the erratic behavior and further im-
prove the selectivity of the spectrometer are being continued, but at the
present stage of development there is much that can be determined con-
cerning the processes of fragmentation of hydrocarbons, since many
fragments apparently are released with energies considerably greater
than this lower limit. Also at some later date the fragmentation yields
and energies will be measured for a wider range of energies of electron
bombardment.

V. THEORETICAL PHYSICS, GENERAL

V-15-12.   Statistical Properties of Nuclear Energy States   (51210-01)

Norbert Rosenzweig

A statistical theory of nuclear forces has been constructed along the same lines as the statistical mechanics of Gibbs. In analogy to the phase space, there is the system space of real symmetric matrices of dimensionality N. This space is our model of the space of all possible physical systems, and the task is to apply sound statistical principles in order to define suitable representative ensembles from which such physical properties as statistics about the eigenvalue structure, neutron width distributions, etc. may be deduced.

Of fundamental importance in the theory is the one-one correspondence which can be defined between the real symmetric matrix H in N dimensions and the same object regarded as a vector in $\frac{1}{2} N(N + 1)$ dimensions in a definite (though unknown) basis. This correspondence may be expressed as

$$\|H_{ij}\| \rightleftharpoons (H_{11}, \sqrt{2}\, H_{12}, \cdots, \sqrt{2}\, H_{1N}, \cdots, H_{NN}) . \quad (1)$$

The volume element in the system space is

$$dV \equiv 2^{\frac{1}{4} N(N - 1)} \prod_{i \leqslant j} dH_{ij} . \quad (2)$$

The system space of the matrices H is unbounded. This makes it impossible to define a normalizable distribution that gives the same weight to every system, unless the magnitude of the matrix elements is restricted in some way.

A somewhat similar situation occurs in the usual statistical mechanics in which, to begin with, the phase space of the Hamiltonian variables is unbounded. It is only when conservation of energy is taken into

account that the relevant part of phase space becomes bounded, and it becomes possible to implement the idea of equal a priori probability in the form of the micro-canonical ensemble. The question therefore arises whether there is a quantity, analogous to the energy in the statistical mechanics of Gibbs, which will restrict the magnitude of the matrix elements in the statistical theory of interactions in a physically significant way.

A paper being prepared for publication advances the notion that there is an analog to energy in the theory under consideration, namely a quantity which characterizes the strength of the interactions of a complex physical system. The average value of the spacing between energy levels would be the natural measure of this strength. However, in the space of real symmetric matrices a more convenient quantity (which turns out to be proportional to the average spacing) is the radius R of the $\frac{1}{2}N(N + 1)$-dimensional sphere in system space, namely

$$R^2 = \text{Spur } H^2 .\tag{3}$$

The idea of restricting attention to systems of a definite strength is justified on the grounds of the general statistical principle that one must incorporate into a statistical theory such knowledge about a system as one has (or can easily obtain).

Physically, restriction (3) is an implementation of the idea that one knows the average spacing between energy levels. One can, for example, observe a few neighboring levels, as is often done, and from this bit of knowledge estimate by extrapolation the density of energy levels over a wide range of energy containing thousands of levels. (The same principle also forces us to take account of conservation of parity and spin, and invariance under time reversal. Previous work has shown that agreement with experiment can be obtained only on this basis.)

The analog of the micro-canonical ensemble is the matrix ensemble E_R defined by the probability density $F(H)$ which is proportional to

$$F(H) \propto \delta \left[\frac{\text{Spur } H^2}{R^2} - 1 \right] . \qquad (4)$$

The ensemble E_R is, in fact, uniquely defined by the condition that it shall be invariant under all mappings of the space T_R of systems of fixed strength onto itself. These mappings, the group of orthogonal transformations $O[\frac{1}{2}N(N + 1)]$, represent our model for an arbitrary change in nuclear forces. (The invariance just discussed is analogous to the invariance of the micro-canonical ensemble of Gibbs under the motion of the phase points produced by a metrically transitive Hamiltonian.)

The ensemble E_R is also invariant under a change of representation of states. An analysis of this question leads to the derivation of the distribution of eigenvalues and the associated ensemble of eigenvectors. The latter is the invariant group measure of $O(N)$.

Wigner's Gaussian ensemble E_G and the new ensemble E_R are related to each other in the same way as the micro-canonical and canonical ensembles are related in the theory of Gibbs. Thus, E_G and E_R have identical statistical properties as $N \rightarrow \infty$. This statement holds not only for the distributions of the vectors H, but also for the eigenvalues of the same objects regarded as matrices through the correspondence (1). Therefore, the consequences of E_R are also in the same good agreement with the experimental data on the distributions of spacings and of neutron widths, and with the dispersion of the gyromagnetic ratios in complex spectra.

V-33-3.   Time Reversal, Flux Quantization, and the Current-Carrying
           State (formerly "Flux Quantization and the Current-Carrying
           State in a Superconducting Cylinder")   (51300-01)

Murray Peshkin

The theory of Byers and Yang[1] explains the quantization of
magnetic flux trapped in a superconducting ring on the basis of four assumptions:

(a) The mutual magnetic interactions of the superconducting electrons
    may be replaced by an external magnetic field, comparable to
    the Hartree field.

(b) The current density and magnetic field are negligible except in a
    narrow region near the surface, as required by the Meissner
    effect. Then, for practical purposes, one deals with a flux
    threading the current loop but confined to the hole.

(c) Appropriate zero-order wave functions for electrons deep in the
    superconductor are antisymmetrized products of independent-
    particle wave functions, the latter having definite canonical
    angular momentum.

(d) Some interaction, such as that of the BCS theory,[2] reduces the
    energy of degenerate independent-particle states enough to pro-
    duce a sufficiently large gap that the flux will adjust itself to
    values which produce degeneracy.

It is shown in this report that assumption (c) above is un-
necessarily restrictive, and that it may be replaced by the alternative
assumption:

---

[1] N. Byers and C. N. Yang, Phys. Rev. Letters 7, 46 (1961).

[2] J. Bardeen, L. N. Cooper, and J. R. Schrieffer, Phys. Rev. 108,
1175 (1957).

(c') Appropriate zero-order wave functions for electrons deep in the

superconductor involve correlations (apart from those induced

by antisymmetrizing) of only a few electrons and/or holes.

Consider first the situation in which zero flux threads the
loop. Time-reversal symmetry imposes a two-fold degeneracy upon all
current-carrying few-particle states. Then according to assumption (d),
zero is a permitted value of the flux. Now a repetition theorem of Peshkin,
Talmi, and Tassie[3] may be used to establish the same two-fold degeneracy
when the flux has the value (in Gaussian units)

$$F_\ell = \ell(2\pi\hbar c/e) \tag{1}$$

for integers ℓ. Thus all integral multiples of $(2\pi\hbar c/e)$ are allowed values
of the flux.

For half-integral values of ℓ, the situation is more compli-
cated. If ψ is a few-particle wave function with $\ell = \frac{1}{2}$, then its time-reversal
partner $\bar{\psi}$ is a few-particle wave function, of the same energy, with $\ell = -\frac{1}{2}$.
The repetition theorem can then be used to generate a wave function $\bar{\psi}'$ with
$\ell = \frac{1}{2}$, which is the time-reversal partner of ψ and is degenerate with it.
From this assertion, which is proved in the Appendix below, it follows that
$\ell = \frac{1}{2}$ (and then, by the repetition theorem, every half-integral value of ℓ) is
allowed.

The approach presented here has three important advantages
over the original one. First, it shows that the allowed values of the flux
are independent of the shape of the superconducting ring, since it does not
require definite angular momentum. Second, it does not require the assump-
tion of strict independent-particle motion in the zero-order approximation.

---

[3] M. Peshkin, I. Talmi, and L. J. Tassie, Ann. Phys. 12, 426 (1961).

Third, it emphasizes that the effective replacement of e by 2e in the flux unit results from the two-fold degeneracy under time reversal, not necessarily from correlated motion of two electrons.

An important sidelight of these considerations deals with the gauge invariance of the BCS theory. In the usual treatment, one couples momentum $\vec{p}$ to $-\vec{p}$ and ignores the possibility that magnetic fields may be present. However, when a current flows there is always a return current and an enclosed flux, so that the vector potential $\vec{A}$ cannot vanish everywhere in the superconducting loop. If the BCS interaction is made gauge invariant by coupling opposite values of $[\vec{p} - (e/c)\,\vec{A}]$, one may wonder whether each state has indeed a partner. Even if it has, the approximation is suspect because the (gauge invariant) enclosed flux is known to influence the motion of electrons. It is now evident that quantizing the flux independently of shape guarantees the flux values for which time-reversal partners exist. The repetition theorem removes the doubt about the approximation depending upon the enclosed flux.

A paper enlarging upon these ideas has been prepared for publication.

APPENDIX

For a flux of ℓ units given by Eq. (1), the vector potential $\vec{A}_\ell$ is given by

$$\vec{A}_\ell = \text{grad } S_\ell \, , \tag{2}$$

where S_ℓ is any multiple-valued scalar function of the coordinates whose change in going once around a closed path which encloses the flux is

$$\Delta S_\ell = F_\ell \, . \tag{3}$$

The velocity operator in the presence of flux F_ℓ is

$$\vec{v}_\ell = \frac{1}{m} \left[\frac{\hbar}{i} \nabla - \frac{e}{c} \vec{A}_\ell \right] . \tag{4}$$

Two wave functions ψ' and ψ, with possibly different flux values ℓ' and ℓ, are time-reversal partners if

$$\left\langle \psi' \middle| f(\vec{x}, \vec{v}, \vec{\sigma}) \middle| \psi' \right\rangle = \left\langle \psi \middle| f(\vec{x}, -\vec{v}, -\vec{\sigma}) \middle| \psi \right\rangle , \tag{5}$$

where f is an arbitrary function of all the electron coordinates, velocities, and spins. Define $\bar{\psi}$ by

$$\bar{\psi} = \psi \exp \left\{ \frac{ie}{\hbar c} \sum_k \left[S_{\ell+1}(\vec{x}_k) - S_\ell(\vec{x}_k) \right] \right\} , \tag{6}$$

where k labels the electrons. Then the repetition theorem shows that $\bar{\psi}$ is a wave function for $(\ell + 1)$ flux units, with the same energy as ψ. Substitution of Eqs. (4) and (6) into (5) shows that $\bar{\psi}$ is the time-reversal partner of ψ'.

V-42-2.   Time Reversal and Superselection (formerly "Geometric Theory of Charge") (51210-01)

H. Ekstein

The previously reported idea[1] that charge and baryon number can be explained on the basis of relativistic symmetry alone has been further developed. The physical meaning of "the time-reversed state" had previously been given only for special "states" which were eigenfunctions of the momentum operators. This is not only physically insufficient, if the symmetry principle for time-reversal is to be valid for any state, but also mathematically objectionable because, strictly speaking, the momentum operators have no nontrivial eigenstates except the vacuum. The present paper gives a reformulation which refers only to proper states, and also to all proper states.

The broadening of the physical statement, together with the removal of a mathematical awkwardness, makes the structure of the theory more perspicuous. As a consequence, it can be seen that three specific postulates on the structure of superselected Hilbert spaces can be replaced by only one postulate which is almost trivially simple: that the algebra of observables is closed. In the present case this means merely that any self-adjoint operator constructed by the operations of multiplication, addition, and multiplication by numbers (applied to observables) is itself an observable.

No new results are obtained, but the results of the previous paper now have a firmer and simpler foundation. This is reported in a paper that has been accepted for publication.[2]

---

[1] H. Ekstein, Physics Division Summary Report ANL-6262 (December 1960), p. 34; Phys. Rev. 120, 1917 (1960).

[2] H. Ekstein, Nuovo cimento (in press).

<u>Meson-Nucleon Interaction</u>   (51151-01)

K. Hiida, M. Soga, and K. Tanaka
Reported by K. Tanaka

TOTAL CROSS SECTIONS AT HIGH ENERGIES

We use a hypothesis of generalized isospin independence to explain three inequalities among the total cross sections at high energies, namely,

$$\sigma(\pi^-, p) > \sigma(\pi^+, p), \tag{1}$$

$$\sigma(K^-, p) > \sigma(K^+, p), \tag{2}$$

and

$$\sigma(\bar{p}, p) > \sigma(p, p). \tag{3}$$

In the case of inequality (1), one may write from charge independence that

$$\sigma(\pi^-, p) - \sigma(\pi^+, p) = \frac{2}{3} \sum_{i}{}_c \left[\sigma^{(i)}(T = \tfrac{1}{2}) - \sigma^{(i)}(T = \tfrac{3}{2}) \right]$$
$$+ \frac{2}{3} \sum_{i}{}_n \sigma^{(i)}(T = \tfrac{1}{2}), \tag{4}$$

where $\sum_c$ and $\sum_n$ are sums over common and noncommon channels, respectively. Final states with the same kinds and same numbers of particles, irrespective of the z components of their isospin T_3, strangeness, and baryon number, are designated as being in the same channel. Use has been made of the fact that $\sigma(\pi^-, p)$ includes all the channels (channel being defined by the kind of particle and its number) that belong to the (π^+, p). The noncommon channels with pure $T = \frac{1}{2}$ that belong to (π^-, p) alone are exhausted by

$$\Lambda + K^0 + m(\Lambda + \bar{\Lambda}),$$

$$n + \Lambda + \bar{\Lambda} + m(\Lambda + \bar{\Lambda}), \qquad (m = 0, 1, 2, \cdots) \tag{5}$$

$$\bar{\Xi}^0 + \Lambda + \Lambda + m(\Lambda + \bar{\Lambda}).$$

Making the dynamical assumption that at high energies

$$\sum_{\substack{i \\ c}} \sigma^{(i)} (T = \tfrac{1}{2}) = \sum_{\substack{i \\ c}} \sigma^{(i)} (T = \tfrac{3}{2}) \tag{6}$$

then leads to the relations

$$\sigma(\pi^-, p) = \sigma(\pi^0, p) = \sigma(\pi^+, n) = \sigma(\pi^0, n) > \sigma(\pi^+, p) = \sigma(\pi^-, n) \tag{7}$$

at high energies.

In a similar manner, the inequalities (2) and (3) are explained on the basis of four facts: (α) the isospin of the Λ particle is zero; (β) all hyperons have strangeness of the same sign ; (γ) the strangeness of all hyperons is negative; and (δ) the pion and kaon have baryon number zero. Inequality (1) was explained by (α), inequality (2) by (α) and (γ), and inequality (3) by (α), (β), and (δ).

Other relations, derived in a similar manner, which may be of experimental interest are

$$\sigma(\pi^+, \pi^-) > \sigma(\pi^+, \pi^+) = \sigma(\pi^-, \pi^-) ,$$

$$\sigma(\Sigma^-, p) = \sigma(\Sigma^+, n) > \sigma(\Sigma^+, p) = \sigma(\Sigma^-, n) ,$$

$$\sigma(\overline{\Sigma}^+, p) = \sigma(\overline{\Sigma}^-, n) > \sigma(\overline{\Sigma}^-, p) = \sigma(\overline{\Sigma}^+, n) ,$$

$$\sigma(\Xi^-, p) > \sigma(\Xi^-, n), \qquad \sigma(\overline{\Xi}^-, p) = \sigma(\overline{\Xi}^-, n) , \tag{8}$$

$$\sigma(\pi^-, d) = \sigma(\pi^+, d) ,$$

$$\sigma(K^-, d) > \sigma(K^+, d) ,$$

$$\sigma(\overline{p}, d) > \sigma(p, d) .$$

A report on this work has been prepared for publication.

PUBLICATIONS SINCE THE LAST REPORT

PAPERS

GROUP THEORY
M. Hamermesh . . . . (Unattached)
Addison-Wesley Publishing Co., Reading, Mass., 1962

HIGH-FREQUENCY PLASMOIDS
A. J. Hatch . . . . (Project IV-10)
Proceedings of the Fifth International Conference on
Ionization Phenomena in Gases, edited by H. Maecker
(North-Holland Publishing Co., Amsterdam, 1962),
Vol. I, pp. 748-755

ABSTRACTS

A GAMMA-RAY SPECTROMETER FOR STUDIES OF RESONANT-CAPTURE GAMMA-RAY SPECTRA
L. M. Bollinger, R. T. Carpenter, R. E. Cote', and
H. E. Jackson . . . . (Project I-7)
Neutron Time-of-Flight Methods, edited by J. Spaepen
(European Atomic Energy Community, Brussels,
September 1961), p. 431

SPIN ASSIGNMENT OF RESONANCES FROM CAPTURE GAMMA-RAY SPECTRA
L. M. Bollinger and R. E. Cote' . . . .(Project I-7)
Neutron Time-of-Flight Methods, edited by J. Spaepen
(European Atomic Energy Community, Brussels,
September 1961), pp. 199-201

GLASS SCINTILLATORS FOR NEUTRON DETECTION
L. M. Bollinger and G. E. Thomas . . . . . . (Project I-2)
Neutron Time-of-Flight Methods, edited by J. Spaepen
(European Atomic Energy Community, Brussels,
September 1961), pp. 431-436

INELASTIC SCATTERING OF α PARTICLES BY Zn^{64} and Zn^{68}
H. W. Broek, T. H. Braid, J. L. Yntema, and B.
Zeidman . . . . (Project I-22)
Bull. Am. Phys. Soc. 7, 82 (January 24, 1962)

THE DECAY OF $_{74}W^{188}$ (65 d) AND $_{75}Re^{188}$ (18 hr)
    S. B. Burson, D. Zei, and T. Gedayloo . . . . . (Project I-36)
    Bull. Am. Phys. Soc. $\underline{7}$, 35 (January 24, 1962)

THE E1 GAMMA-RAY STRENGTH FUNCTION FOR $144 \leqslant A \leqslant 202$
    R. T. Carpenter and L. M. Bollinger . . . . . (Project I-7)
    Bull. Am. Phys. Soc. $\underline{7}$, 10 (January 24, 1962)

ANALYSIS OF RESONANT-CAPTURE γ-RAY SPECTRA . .(Project I-7)
    R. T. Carpenter, J. P. Marion, and L. M. Bollinger
    Neutron Time-of-Flight Methods, edited by J. Spaepen
    (European Atomic Energy Community, Brussels,
    September 1961), pp. 563-564

LOW-LYING LEVELS IN Hg^{200}
    R. T. Carpenter, R. K. Smither, and R. E. Segel . .(Project I-60)
    Bull. Am. Phys. Soc. $\underline{7}$, 11 (January 24, 1962)

MÖSSBAUER EFFECT IN Gd^{155}
    C. Littlejohn Herzenberg, L. Meyer-Schutzmeister, L. L.
    Lee, Jr., and S. S. Hanna . . . . (Project I-19)
    Bull. Am. Phys. Soc. $\underline{7}$, 39 (January 24, 1962)

ELASTIC NUCLEON-NUCLEON SCATTERING AT HIGH ENERGIES
AND SMALL ANGLES
    K. Hiida . . . . (Project V-46)
    Bull. Am. Phys. Soc. $\underline{7}$, 40 (January 24, 1962)

ISOTOPIC IDENTIFICATION OF RESONANCES FROM CAPTURE
GAMMA-RAY SPECTRA
    H. E. Jackson and L. M. Bollinger . . . . . . (Project I-7)
    Neutron Time-of-Flight Methods, edited by J. Spaepen
    (European Atomic Energy Community, Brussels,
    September 1961), pp. 191-197

TEMPERATURE SHIFT IN THE MÖSSBAUER SPECTRUM OF
METALLIC IRON . . . . (Project I-19)
    R. S. Preston, J. Heberle, T. R. Hart, and S. S. Hanna
    Bull. Am. Phys. Soc. $\underline{7}$, 39 (January 24, 1962)

STATISTICAL MECHANICS OF EQUALLY LIKELY QUANTUM
SYSTEMS
    N. Rosenzweig . . . . (Project V-15)
    Bull. Am. Phys. Soc. $\underline{7}$, 91 (January 24, 1962)

$Hf^{177}(n,\gamma)Hf^{178}$ AND THE ASSOCIATED ENERGY LEVELS IN Hf^{178}
R. K. Smither . . . . (Project I-60)
Bull. Am. Phys. Soc. 7, 11 (January 24, 1962)

LESSONS LEARNED FROM A CHOPPER ACCIDENT
G. E. Thomas, R. E. Cote', and L. M. Bollinger . . (Project I-1)
Neutron Time-of-Flight Methods, edited by J. Spaepen
(European Atomic Energy Community, Brussels,
September 1961), pp. 297-300

CAPTURE OF ALPHA PARTICLES BY Mg^{24}
J. A. Weinman, L. L. Lee, Jr., L. Meyer-Schutzmeister,
and S. S. Malik . . . . (Project I-16)
Bull. Am. Phys. Soc. 7, 72-73 (January 24, 1962)

Proceedings of the Rutherford Jubilee International Conference,
Manchester, 1961, edited by J. B. Birks (Heywood and Co., Ltd.,
London, 1961)

ANGULAR CORRELATIONS IN INELASTIC SCATTERING OF PROTONS
FROM Mg^{24}
T. H. Braid, J. L. Yntema, and B. Zeidman . . (Project I-22)
pp. 519-520

ELASTIC AND INELASTIC SCATTERING OF 43-MeV α PARTICLES
IN THE Ni REGION . . . . (Project I-22)
H. W. Broek, T. H. Braid, J. L. Yntema, and B. Zeidman
pp. 517-518

STUDIES OF (d,t) REACTIONS ON THE ISOTOPES OF NICKEL
M. H. Macfarlane, B. J. Raz, J. L. Yntema, and
B. Zeidman . . . . (Project I-22)
pp. 511-512

THE (α,t) REACTION ON NUCLEI
J. L. Yntema . . . . (Project I-22)
pp. 513-514

THE (d,He^3) REACTION NEAR Z = 28 . . . . (Project I-22)
J. L. Yntema, T. H. Braid, B. Zeidman, and H. W. Broek
pp. 521-522

Rutherford Jubilee International Conference (continued)

ENERGY DEPENDENCE OF THE B^{10} (d,p) B^{11} ANGULAR DIS-
TRIBUTION
        B. Zeidman, J. L. Yntema, and G. R. Satchler . .(Project I-22)
        pp. 515-516

CONFERENCE SUMMARY
        D. R. Inglis . . . .(Unattached)
        pp. 837-845

ANL TOPICAL REPORT

WEATHER MODIFICATION
        M. B. Rodin and D. C. Hess . . . .(Project VI-1)
        Argonne National Laboratory topical report ANL-6444
        (December 1961)

ADDITIONAL PAPERS ACCEPTED FOR PUBLICATION

POLARIZATION OF NEUTRONS IN SCATTERING FROM LIGHT
NUCLEI AND IN THE Li^7 (p,n) Be^7 REACTION
        A. J. Elwyn and R. O. Lane . . . . (Project I-18)
        Nuclear Phys. (February 1962)

ELASTIC NUCLEON-NUCLEON SCATTERING AT HIGH ENERGIES
AND SMALL ANGLES
        K. Hiida . . . .(Project V-46)
        Phys. Rev. Letters (February 1, 1962)

GEOMETRICAL CONSIDERATIONS IN THE MEASUREMENT OF THE
RATIO L/R IN THE SCATTERING OF POLARIZED NUCLEONS
        J. E. Monahan and A. J. Elwyn . . . . (Project I-18)
        Nuclear Instr. and Methods (March 1962)

PERSONNEL CHANGES IN THE ANL PHYSICS DIVISION
NEW MEMBERS OF THE DIVISION

Staff Member

Mr. John Robert Marquart. Born in Benton Harbor, Michigan, 1933.
Home address: 5009 Wilcox, Downers Grove, Illinois.
B.S., University of Arizona, 1955; M.S., University of
Illinois, 1961. He joined the Physics Division on January
22, 1962 to work on the mass spectrometry of inorganic
polymers.

Technician

Mr. Gordon Goodwin joined the Physics Division on January 22, 1962
as a Research Technician (Junior) with M. Kaminsky.